

Definition of graphic signatures for solid surface vibrations

Leonardo Guimarães Aleixo¹

¹Federal University of Pará, Belém/Pará - Brazil

Abstract—This research brings together the study of mathematical models for predicting numerical patterns and graphic signatures on the impulse response of vibrations. The gathered data collection receives computational processing analysis, with the application of functions that define the linearity of the set of values and obtains the polynomial response for the signal amplitude. The Meta-heuristic defines non-deterministic behavior through Tabu-Search optimization, dispersion response by data limits and finally defining the impulse stability of the samples.

Keywords—Optimization, vibration, modeling.

I. INTRODUCTION

The geometry of numerical data defines shapes and signatures, in response to new mathematical models for the processing of mechanical vibrations that occur in different solid surfaces and in regions that present resistance to external forces. The present work presents the application of polynomial and optimized methods to the developed computational system, coupled to surface-adhered sensors for the return of computational impulse values processing. The combination of a simple embedded system and mathematical modeling returns three graphical analyzes with definition of strength and resistance patterns, and with graphic projection of dispersion. Simple circuit and computational analysis with enough flexibility allow the engineer and the student to build an embedded system creating a solid base through numerical method and signal processing. The study carried out in [1] informs that heuristic algorithms do not guarantee to find the optimal solution for a given problem, however, they are able to improve an existing solution by returning a viable answer with quality in a reasonable time. The Meta-heuristic described in [2] demonstrates and expands event response possibilities using algorithms and compiling optimization concepts in programming.

According to [3] the computerized system called *Arduino Uno* is based on the microcontroller *ATmega328*², and which essentially uses a standard programming language *C/C++*. [4] describes the *Arduino IDE* as a cross-platform application for *software* development, using a code editor to program input and output operations. The sensor used according to [5], is a device that responds to the *physical/chemical* stimulus in a specific way, and can be transformed into physical quantity for measurement and monitoring purposes defined as a transducer, or meter. Being able to convert type of energy where the resistance variation is read and then processed to obtain the desired information. For the study of vibrations as

demonstrated by [6], forces on surfaces of visible objects are returned through the effect of sound or unidentified force, being recorded by high-speed video cameras. An attempt was made in [7] to estimate the seismic energy dissipated for different distances from the explosion site, using signal processing techniques supported by a programmable computerized system. The development of portability and low cost equipment is studied in [8] with feedback of vibration values for a data collection network in a wide geographic area.

II. META HEURISTIC

A. Graham Scan

Optimization applied to numerical values and signal processing returns and defines graphical behavior patterns, encompassing the non-deterministic study in modeling seismic impulses detected on solid surfaces. In this research, the meta-heuristic applies mathematics as data science to engineering and obtains a graphical response. Algorithm 1 performs the Graham-Scan scan and with the example seen in Fig. 1, through the computational code³ written in Python. It was adapted to force analysis within a total set of seismic values. Solving the convex hull problem in the generation of graphic traverse containing vertices for contour lines. The numerical importance lies in combining reading points that can form closed paths, allowing the convex analysis of the processed data from the sensor and thus being able to display the graphic-geometric behavior of the distribution of the samples. As seen in [9] a convex analysis algorithm is applied that takes advantage of the geometric and symmetric advantages of quadrants formed in 2D spaces. The application in [10] uses a convex method that seeks to define polygonal geometry through dispersed points with reduced complexity of dispersion limits.

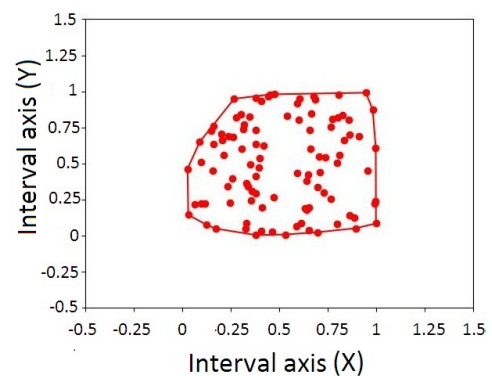


Fig. 1. Convex polygon for random numbers

leotelecom@bol.com.br, <https://orcid.org/0000-0002-1825-934X>.

¹<https://store.arduino.cc/usa/arduino-uno-rev3>.

²<https://pt.wikipedia.org/wiki/ATmega328>

³<https://gist.github.com/yumka/dfce90b51e4e31576ec5>

Algorithm 1: GRAHAM-SCAN(Q)

```

1 begin
2   Let  $p_0$  be the point in  $Q$  with minimum coordinate  $y$  or such a point
   that is
3   most to the left in case of a tie
4   Let  $(p_1, p_2, \dots, p_n)$  be the remaining points in  $Q$ , sorted by polar angle
   in counterclockwise order around  $p_0$ , where if hover more
5   than a point with the same angle, all points are removed, except
6   the farthest from  $p_0$ 
7   Let  $S$  be an empty stack
8   Move( $p_0, S$ )
9   Move( $p_1, S$ )
10  if  $m \geq 2$  Move( $p_2, S$ ) then
11    for  $i = 3$  to  $m$  do
12      while the angle formed by the points Near Top( $S$ ), Top( $S$ ) and
13         $p_i$  curve does not turn left do
14          Stacks)
15        end
16        Move( $p_i, S$ )
17      end
18    end
19  end
20 return  $S$ 
    
```

B. Tabu Search

It is also important to obtain patterns of graphical and numerical composition that predict behaviors of processed signals, with mathematical exploration beyond deterministic models. As a parallel study to the probabilistic calculation, the Algorithm 2 *Tabu Search* was applied, adapted for the knapsack problem, in the analysis of numerical data in vibrations. The tabu search metaheuristic tries to return a memory management scheme that reduces the possibility of examining the same configuration or problem solution more than once (S). The set of prohibitions of the algorithm is registered in a dynamic memory that allows its alteration according to the progress of the search and other circumstances, employing strategies that prohibit actions or search movements, starting from choices of solutions that explore the neighborhood of data. The strategy of searching for solutions through the knapsack problem will define the numerical values of vibrations that approach the average value, using a decision variable with applications of restrictions seen in (13) section V-A.

Algorithm 2: TABU SEARCH

```

1 Generate an initial solution  $S$ , and do  $S^* := S$ 
2 Initialize Tabu List ( $T$ ) and counters  $p$  and  $q$ 
3 begin
4   While  $p \neq p_{max}$  and  $q \neq q_{max}$  Do it
5   begin
6     Select the best neighbor  $S' \in N(S) \setminus T$ 
7     Select the best neighbor  $S'' \in N(S) \cap T$ 
8     begin
9       If  $f(S'') < f(S')$  and  $f(S'') < f(S^*)$  then
10         $S' \leftarrow S''$ 
11      If  $f(S') < f(S^*)$  then
12         $S^* \leftarrow S'$ 
13         $q \leftarrow 0$ 
14      If  $f(S') < f(S)$  then
15        put the inverse move ( $S', S$ ) in list  $T$  and update  $T$ 
16         $S \leftarrow S'$ 
17         $p \leftarrow p + 1$ 
18         $q \leftarrow q + 1$ 
19      end
20    end
21  end
22 Exit with the solution  $S^*$ , for an optimized set of filters digital signals in a
   signal transmission network.
    
```

III. CASE STUDY

The graphic signature is defined by mathematical models through data collection and signal processing. Computerized plate receives vibration signals converting to electrical pulses and numerical values seen in IV, obtaining graphical samples compared to linearity and polynomial analysis. The second stage, seen in V, analyzes optimized solutions of vibration impulses, returning graphs for defining the convex perimeter of samples, together with the analysis of numerical stability of values for automation.

IV. SIGNAL PROCESSING

The basic circuit was used in the association of Wheatstone bridge⁴ containing three resistors of values $R_2=175.4$ (Ohms), $R_4=221.8$ (Ohms), $R_3=221.8$ (Ohms) and the sensor $RS=$ Strain Gauge. The readings obtained are accurately processed in numerical format of sixteen decimal places, seeking to increase accuracy in signal analysis. The processed result presents 29 interval readings every three seconds, for the values of time, charge and deformation. The charge will display variable voltage values emitted by the **Strain Gauge** which is connected to logic port A0 of the Arduino UNO board, which are normalized to a maximum of 5 volts output. For Deformation, charge values will be displayed on a microstrain scale⁵ calculated by (3), where S is the sensitivity factor of **Strain Gauge** and indicating deformation in (3) according to [11]. We also have parameters E_i of values in voltage (v) for the source external to the strain gauge, and the E_0 in (1) assumes a variable value obtained by the Arduino UNO board. The result of collected samples can be seen in Table I.

$$\frac{E_o}{E_i} = \frac{S \cdot \varepsilon \cdot 10^3}{4} \cdot \left[\frac{2}{2 + S \cdot \varepsilon \cdot 10^6} \right] \quad (1)$$

$$\frac{\Delta R}{R} = S \cdot \varepsilon \quad (2)$$

$$\varepsilon = \frac{1}{S \cdot 10^3} \cdot \left[-\frac{16 \cdot E_o}{(8 \cdot E_o) - E_i} \right] \quad (3)$$

 TABLE I
 SIGNAL SAMPLING

Time (seconds)	First Reading		Second Reading		Third Reading	
	charge 1	Deformation 1	charge2	Deformation 2	charge 3	Deformation 3
3	0.0048875855	0.0000120052	0.0049019608	0.0000120409	0.0048875855	0.0000120052
6	0.0048971596	0.0000120290	0.0049067713	0.0000120529	0.0049067713	0.0000120529
9	0.0048875855	0.0000120052	0.0048971596	0.0000120290	0.0048875855	0.0000120052
12	0.0048971596	0.0000120290	0.0048875855	0.0000120052	0.0048971596	0.0000120290
15	0.0048923679	0.0000120171	0.0048875855	0.0000120052	0.0048923679	0.0000120171
18	0.0048875855	0.0000120052	0.0048875855	0.0000120052	0.0048971596	0.0000120290
21	0.0048971596	0.0000120290	0.0048971596	0.0000120290	0.0048875855	0.0000120052
24	0.0048923679	0.0000120171	0.0048875855	0.0000120052	0.0049019608	0.0000120409
30	0.0049067713	0.0000120529	0.0048923679	0.0000120171	0.0048875855	0.0000120052
33	0.0048971596	0.0000120290	0.0048875855	0.0000120052	0.0049019608	0.0000120409
36	0.0049019608	0.0000120409	0.0048923679	0.0000120171	0.0048971596	0.0000120290
39	0.0049019608	0.0000120409	0.0049019608	0.0000120409	0.0048875855	0.0000120052
42	0.0048971596	0.0000120290	0.0048875855	0.0000120052	0.0049019608	0.0000120409
45	0.0048923679	0.0000120171	0.0049067713	0.0000120529	0.0048875855	0.0000120052
48	0.0048875855	0.0000120052	0.0048971596	0.0000120290	0.0048971596	0.0000120290
51	0.0048875855	0.0000120052	0.0048875855	0.0000120052	0.0048923679	0.0000120171
54	0.0048875855	0.0000120052	0.0048875855	0.0000120052	0.0049019608	0.0000120409
57	0.0049019608	0.0000120409	0.0048875855	0.0000120052	0.0048875855	0.0000120052
60	0.0048971596	0.0000120290	0.0048875855	0.0000120052	0.0048875855	0.0000120052
63	0.0049019608	0.0000120409	0.0048875855	0.0000120052	0.0049019608	0.0000120409
66	0.0049019608	0.0000120409	0.0048875855	0.0000120052	0.0048971596	0.0000120290
69	0.0048875855	0.0000120052	0.0048971596	0.0000120290	0.0048875855	0.0000120052
72	0.0049019608	0.0000120409	0.0048923679	0.0000120171	0.0048923679	0.0000120171
75	0.0048971596	0.0000120290	0.0049019608	0.0000120409	0.0048875855	0.0000120052
78	0.0049019608	0.0000120409	0.0048971596	0.0000120290	0.0048875855	0.0000120052
81	0.0048875855	0.0000120052	0.0049019608	0.0000120409	0.0048875855	0.0000120052
84	0.0049019608	0.0000120409	0.0048971596	0.0000120290	0.0049019608	0.0000120409
87	0.0048875855	0.0000120052	0.0048971596	0.0000120290	0.0048923679	0.0000120171
90	0.0049019608	0.0000120409	0.0048923679	0.0000120171	0.0049067713	0.0000120529
Average	0.00489551	0.00001203	0.00489386	0.00001202	0.00489419	0.00001202
Variance	$3.869 \cdot 10^{-38}$	$2.361 \cdot 10^{-40}$	$9.0385 \cdot 10^{-35}$	$2.0089 \cdot 10^{-41}$	$5.3 \cdot 10^{-36}$	$3.7 \cdot 10^{-41}$
Standard deviation	$1.966 \cdot 10^{-19}$	$1.536 \cdot 10^{-20}$	$9.507 \cdot 10^{-18}$	$4.48208 \cdot 10^{-21}$	$2.3 \cdot 10^{-18}$	$6.1 \cdot 10^{-21}$

⁴Schematic for the measurement of unknown electrical resistance.

⁵Magnitude of deformation $\varepsilon \cdot 10^{-6} (\mu\varepsilon)$.

A. Linearity functions

Being able to understand the linearity of numerical behavior goes back to research for the prediction of deterministic models. In the practice of empirical calculus, value responses follow little rules and prediction patterns, but still may contain within their datasets deterministic point clusters that can be formulated. The equations (4), (5), (6), (7), (8) and (9) were modeled from the samples (12, 15, 18), (36, 39, 42) and (81, 84, 87) seen in Table II, seeking to define the existence of several linear and non-linear points that can obtain answers charts on a standardized scale of 29, as a basis for building a definition of mathematical modeling.

TABLE II
SAMPLES OF FUNCTIONS

Time (seconds)	First Reading		Second Reading		Third Reading	
	charge 1	Deformation 1	charge2	Deformation 2	charge 3	Deformation 3
	P_{C1}		P_{D1}			
12	0.0048971596	0.0000120290				
15	0.0048923679	0.0000120171				
18	0.0048875855	0.0000120052				
			P_{C2}		P_{D2}	
36			0.0048923679	0.0000120171		
39			0.0049019608	0.0000120409		
42			0.0048875855	0.0000120052		
			P_{C3}		P_{D3}	
81			0.0048875855	0.0000120052		
84			0.0049019608	0.0000120409		
87			0.0048923679	0.0000120171		

Defined equations:

$$P_{C1}(x) = +4,65 \cdot 10^{-9}x^2 - 4,81 \cdot 10^{-6}x + 49,02 \cdot 10^{-4} \quad (4)$$

$$P_{D1}(y) = -8,47 \cdot 10^{-22}y^2 - 1,19 \cdot 10^{-8}y + 12,04 \cdot 10^{-6} \quad (5)$$

$$P_{C2}(x) = -11,98 \cdot 10^{-6}x^2 + 45,54 \cdot 10^{-6}x + 48,59 \cdot 10^{-4} \quad (6)$$

$$P_{D2}(y) = -2,98 \cdot 10^{-8}y^2 + 1,13 \cdot 10^{-7}y + 11,93 \cdot 10^{-6} \quad (7)$$

$$P_{C3}(x) = -11,98 \cdot 10^{-6}x^2 + 50,33 \cdot 10^{-6}x + 48,49 \cdot 10^{-4} \quad (8)$$

$$P_{D3}(y) = -2,98 \cdot 10^{-8}y^2 + 1,25 \cdot 10^{-7}y + 11,91 \cdot 10^{-6} \quad (9)$$

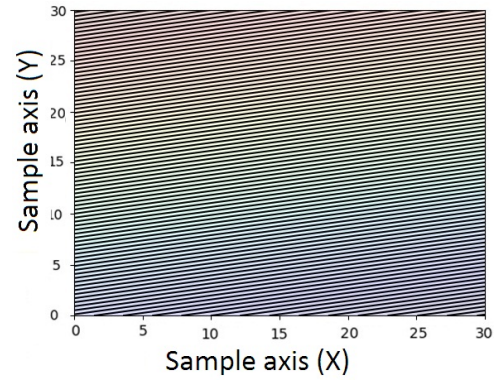
B. Graphic equations

The linearity and impulse response behavior were summarized through (10), (11) and (12), with non-linear graphical visualization in Fig. 2(b) and Fig. 2(c), but Fig. 2(a) shows linear pattern within the scale of 29 samples. The images bring non-linear and linear grouping responses that are inserted in a larger set of numerical samples, which brings a vision of the behavior in scale of what is possible to predict or not within the physical vibration data. The characteristics of data collection come from the wooden surface with information obtained through a single sensor and by periodic impulses in time.

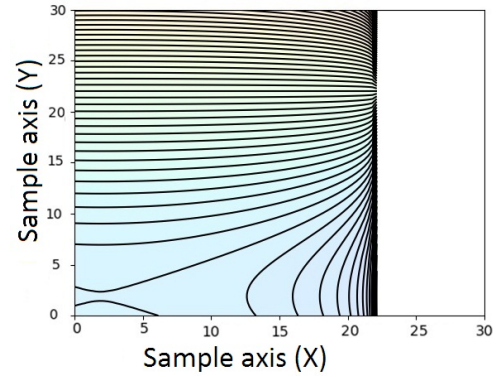
$$H_1(x,y) = [P_{C1}(x)]^{P_{D1}(y)} \quad (10)$$

$$H_2(x,y) = [P_{C2}(x)]^{P_{D2}(y)} \quad (11)$$

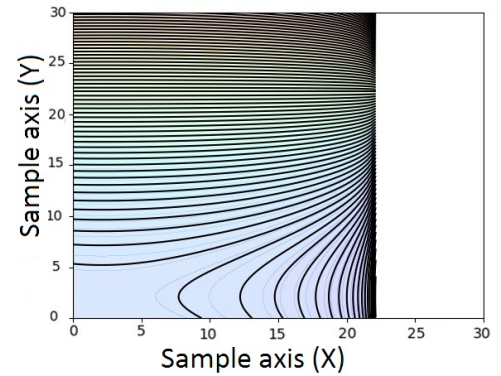
$$H_3(x,y) = [P_{C3}(x)]^{P_{D3}(y)} \quad (12)$$



(a)



(b)



(c)

Fig. 2. In (a) it presents the result of (10). For (b) the result of (11) is seen. In (c) we have the result of (12).

C. General polynomials

Polynomial models are used in several deterministic applications ranging from linear progression methods to industrial automation equations. For the application in this work, the set of samples presents an important graphic behavior with impulses propagated in the reading time, demonstrating the amplitude of the signal read in a single sensor coupled to the computerized board.

Numerical data are modeled in a deterministic polynomial equation, and the overlapping behavior of responses to charge and strain impulses can be visualized. We see in Fig. 3 central approximation of charge values, and in Fig. 4 we also have Approximate strain values. The values tend to approximate, since the contact surfaces are close, however, some points of the model curve seek to differentiate values, but still within a stable set of readings.

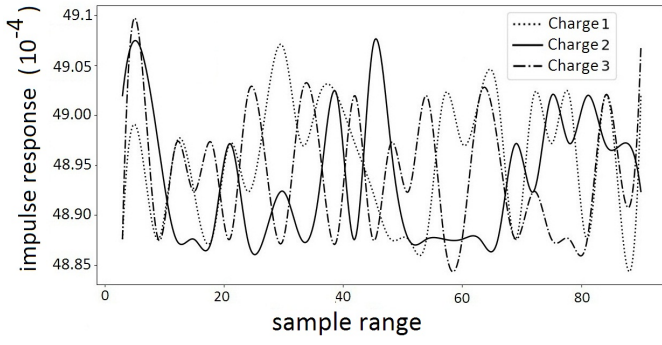


Fig. 3. Impulse response samples for applied charge.

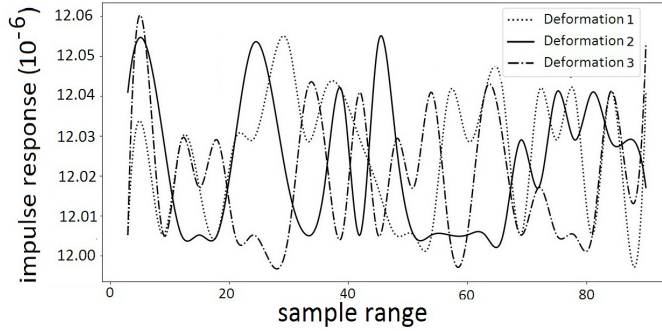


Fig. 4. Impulse response samples for deformation.

V. OPTIMIZATION

A. Optimal vibration values

The set of charge[weight] and deformation[benefit] impulses are optimized to the average value of the 29 charge samples, searching for new numerical solutions of surface data. Where **0** represents the absence of impulse and **1** defines numerical value accepted as solution. The Solution Chain Definition will be able to extend several models of linear systems with varied data in set of solutions defined by the team or by the project developer. The solution for a set of values must approach the average charge value and considering its value in deformation, defined by programming in computational code from the decision variable with restrictions defined and compiled in (13). The set of prohibitions of the algorithm is registered in a dynamic memory that allows its alteration according to the progress of the search and other circumstances, and the results of the iterations can be seen in Table III.

Decision variable:

$$\mathbf{B}_i, \text{ where } i = 1, 2, \dots, 29$$

Constraint for the average value limit:

$$0 \leq \mathbf{B}_i < \approx \text{charge average value}$$

Objective function for optimal solution:

$$S_n = \left[\prod_{j=0}^V (\text{Weight}) \right] \cdot \left[\text{Max} \left(\sum_{i=1}^V \text{solution}[j] \cdot \mathbf{B}_i \right) - \mathbf{B}_{\text{Max}} \right] \quad (13)$$

 TABLE III
OPTIMIZED VIBRATIONS

Time (seconds)	charge and Deformation (1)						charge and Deformation (2)						charge and Deformation (3)					
	Iterations						Iterations						Iterations					
	1	2	3	4	5	6	1	2	3	4	5	6	1	2	3	4	5	6
3	1	1																
6																		
9	1	1	1															
12	1	1	1	1														
15					1													
18	1	1	1															
21				1														
24	1																	
30					1													
33	1	1	1	1														
36	1																	
39	1	1	1	1														
42	1	1	1	1														
45	1	1	1	1														
48	1	1	1	1														
51	1	1	1	1														
54	1	1	1	1														
57	1	1	1	1														
60	1	1	1	1														
63	1	1	1	1														
66	1	1	1	1														
69	1	1	1	1														
72	1	1	1	1														
75	1	1	1	1														
78	1	1	1	1														
81	1	1	1	1														
84	1	1	1	1														
87	1	1	1	1														
90	1	1	1	1														

B. Definition of perimeter and dispersion

Convex analysis was applied to the set of impulses for charge and strain in a total of twenty-nine coordinates with convex projections. You can visualize the maintenance of the midpoint in the prediction of approximate values between the readings for the presented traverses: Fig. 5, Fig. 6, Fig. 7. With demonstration of approximate vertexes and transversal geometry, with linearity of points in the central diagonal of the image.

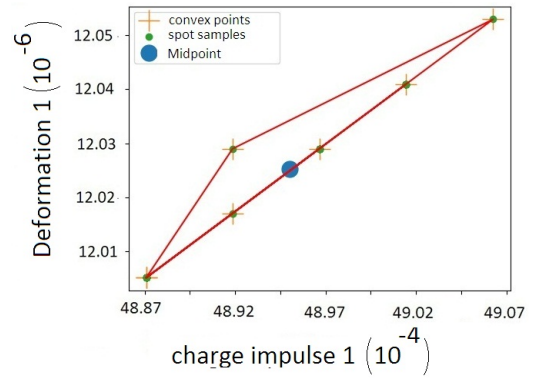


Fig. 5. Convex polygon for charge 1 by Deformation 1.

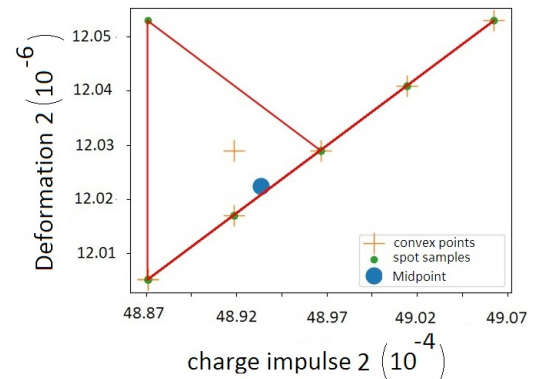


Fig. 6. Convex polygon for charge 2 by Deformation 2

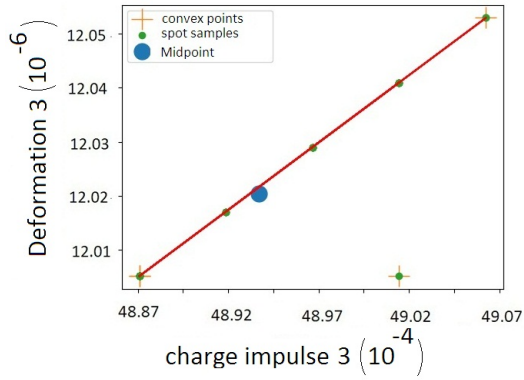


Fig. 7. Convex polygon for charge 3 by Deformation 3

C. Vibration stability

The study of control systems in engineering can use several methods in modeling numerical sets, such as transfer functions and state diagrams. We see that in [12] it is possible to understand and predict the operation of various devices, both mechanical and electrical from small to large portability, with demonstration of simple models that can be coupled to complex controls. The determination of Poles and Zeros, through the transfer function polynomial roots, can predict and anticipate the stability of a dynamic control. The Zeros can modify the coefficients of the exponential terms, while the Poles will identify the classes of signals contained in the impulse response, with these two characteristics these two parameters will graphically predict the stability of a numerical system of samples and simulate the control base complex in vibrations.

Two codes written in Python computational code will perform two analysis steps, the first will be to determine the transfer function⁶ of the values contained in the Tables IV, V and VI, containing three positions for sampled values and linked to intervals of reading times. They are obtained from the polynomial coefficients and the determination of the roots also⁷ that will determine the Poles and Zeros. The Python function `signal.ss2tf` has representation in (14) and (15), which indicate models of a simplified state system and serve as a basis for building diagrams in automation. The purpose of the function is to return the coefficients of the transfer function, being applied to the three sets of charge samples, obtained at different intervals from the total impulses measured by the equipment.

The graphical results can be seen in Fig. 8(a) and Fig. 8(b), where the poles and zeros coincide on the negative side of the real value axis, demonstrating minimum stability in the samples. We can see in Fig. 8(c) that the positions of the poles and zeros are aligned to the real axis of origin, demonstrating a minimal but gradual decrease in the stability of the system.

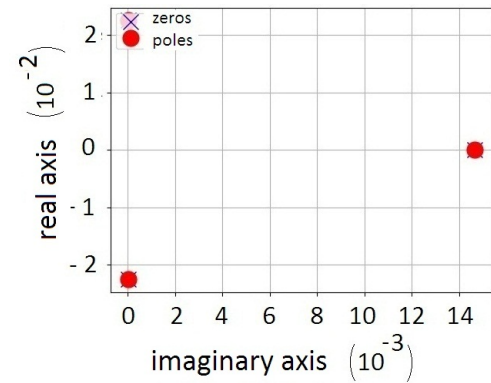
$$\dot{\mathbf{x}}(t) = \begin{bmatrix} C_{11} & C_{12} & C_{13} \\ C_{21} & C_{22} & C_{23} \\ C_{31} & C_{32} & C_{33} \end{bmatrix} \mathbf{x}(t) + \begin{bmatrix} 0 \\ 0 \\ 0 \end{bmatrix} \mathbf{u}(t) \quad (14)$$

$$\mathbf{y}(t) = \begin{bmatrix} M_1 & M_2 & M_3 \end{bmatrix} \mathbf{x}(t) + \begin{bmatrix} 1 \end{bmatrix} \mathbf{u}(t) \quad (15)$$

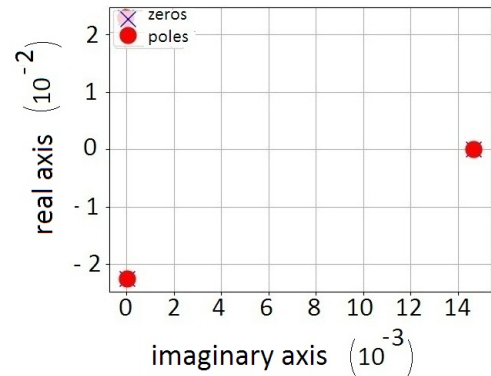
Time(s)	Charge 1	Charge 2	Charge 3	Average
12	0,0048971596	0,0048875855	0,0048971596	0,0048939683
15	0,0048923679	0,0048875855	0,0048923679	0,0048907738
18	0,0048875855	0,0048875855	0,0048971596	0,0048907769

Time(s)	Charge 1	Charge 2	Charge 3	Average
36	0,0049019608	0,0048923679	0,0048971596	0,0048971628
39	0,0049019608	0,0049019608	0,0048875855	0,0048971690
42	0,0048971596	0,0048875855	0,0049019608	0,0048955687

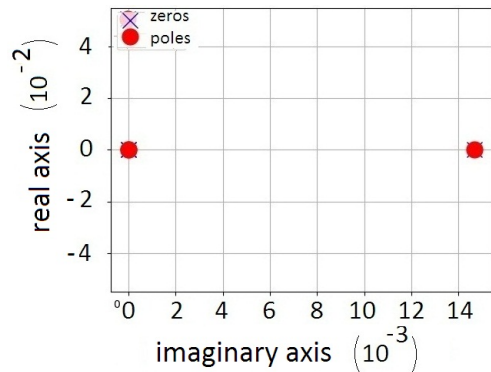
Time(s)	Charge 1	Charge 2	Charge 3	Average
81	0,0048875855	0,0049019608	0,0048875855	0,0048923773
84	0,0049019608	0,0048971596	0,0049019608	0,0049003604
87	0,0048875855	0,0048971596	0,0048923679	0,0048923710



(a)



(b)



(c)

Fig. 8. In (a) we see the stability diagram for Table IV. For (b) it is Stability diagram is shown for the data in Table V. Since (c) demonstrates stability diagram referring to Table V.

⁶<https://docs.scipy.org/doc/scipy/reference/generated/scipy.signal.ss2tf.html>
⁷<https://docs.scipy.org/doc/scipy/reference/generated/scipy.signal.tf2zpk.html>

VI. RESULT AND APPLICATION

The microcontroller board *Arduino UNO* is attached to the computer so that electrical signals emitted by vibrations from the deformation of the sensor *Strain Gauge* are calculated. The geometric analyzes presented from the processed numerical data return joint and graphic behavior of the intensity of impulses, stability and control of values, and even form a polygonal with vertices of peripheral vibrations. As the embedded system obtains and processes samples by sensors, visual patterns are formed, proving the expansion of mathematical modeling by computational means. Deterministic polynomial modeling defines the intensity and oscillatory nature of vibrations, which together with dispersion and convex distribution analyses, and through a few samples, it is possible to define the basis of an impulse response behavior signature on a solid surface. A simplified embedded system of small size and easy to transport, reducing the cost of programmable computing, allowing the numerical analysis of data by a basic circuit connected to a computerized board, together with mathematics that will expand models of signal processing.

VII. CONCLUSION

The work returns analysis for the prediction of optimized models, presenting the assembly of embedded equipment for the processing of force signals on solid surfaces, obtained by sensors and impulse samples, with Improvements in the accuracy of readings through mathematical equations. The study of numerical data demonstrates the linearity of values with distribution of charge matrices and also presents the portability of low-cost equipment. Simulated results and graphs are presented geometrically to define patterns of dispersion of values, using samples of data processed by computerized circuit. The return of stability for a few samples proves wide application for a larger set of numerical data. An increase in points in an optimized network of embedded microcontrollers is suggested, with programmed connection in computerized systems and connected to digital panels for the expansion of the academic network in the study of seismography, civil engineering and aerospace engineering.

REFERENCES

- [1] A. P. da Silva and N. de Oliveira, "Busca tabu e o problema de roteamento de veículos: Uma aplicação prática no exército brasileiro," *RICAM Revista Interdisciplinar de Ciências Aplicadas à Atividade Militar*, ISSN: 13085784, v. 2, n. 2, p. 119-114, (2008), <http://www.ebrevistas.eb.mil.br/RICAM/article/view/2768>.
- [2] E. Goldbarg, M. Goldbarg, and H. Luna, *Otimização combinatória e meta-heurística: algoritmos e aplicações*, 1st ed. Brazil: GEN LTC, 2021.
- [3] UNO, "Arduino," <http://https://www.arduino.cc/en/hardware>, , Brazil, (2019).
- [4] IDE, "Arduino," <https://pt.wikipedia.org/wiki/Arduino>, , Brazil, (2019).
- [5] Sensor, "online," <https://pt.wikipedia.org/wiki/Sensor>, , Brazil, (2019).
- [6] P. Khatri, S. Kadge, and U. Chhatre, "Review of different applications using visual vibration analysis," in *2020 International Conference on Convergence to Digital World - Quo Vadis (ICCDW)*, 2020, pp. 1–4.
- [7] V. R. Sastry and G. R. Chandra, "Assessment of seismic energy obtained from blast induced ground vibrations using signal processing computation techniques," in *2016 IEEE International Conference on Recent Trends in Electronics, Information Communication Technology (RTEICT)*, 2016, pp. 31–35.
- [8] P. Pierleoni, S. Marzorati, C. Ladina, S. Raggiunto, A. Belli, L. Palma, M. Cattaneo, and S. Valenti, "Performance evaluation of a low-cost sensing unit for seismic applications: Field testing during seismic events of 2016-2017 in central Italy," *IEEE Sensors Journal*, vol. 18, no. 16, pp. 6644–6659, 2018.
- [9] A. Beltran and S. Mendoza, "Symmetric hull: A convex hull algorithm based on 2d geometry and symmetry," *IEEE Latin America Transactions*, no. 8, pp. 2289–2295, 2018.
- [10] J. Xu, Z. Zheng, Y. Feng, and X. Qing, "A concave hull algorithm for scattered data and its applications," in *2010 3rd International Congress on Image and Signal Processing*, vol. 5, 2010, pp. 2430–2433.
- [11] D. Dewantara and P. Sasmoko, "Alat penghitung berat badan manusia dengan standart body mass index (bmi) menggunakan sensor charge cell berbasis arduino mega 2560 r3," *GEMA TEKNOLOGI*, no. 3, pp. 100–104, 2015.
- [12] G. F. Franklin, *Sistemas de controle para engenharia*, 6th ed. Bookman, 2013.